ISSN 1062-8738, Bulletin of the Russian Academy of Sciences. Physics, 2015, Vol. 79, No. 9, pp. 1106–1112. © Allerton Press, Inc., 2015.
Original Russian Text © S.V. Salikhov, A.G. Savchenko, I.S. Grebennikov, E.V. Yurtov, 2015, published in Izvestiya Rossiiskoi Akademii Nauk. Seriya Fizicheskaya, 2015, Vol. 79, No. 9, pp. 1251–1258.

Phase Composition and Structure of Iron Oxide Nanopowders Prepared by Chemical Means

S. V. Salikhov[a], A. G. Savchenko[a], I. S. Grebennikov[a], and E. V. Yurtov[b]

[a] *National Research Technological University (MISiS), Moscow, 119049 Russia*
[b] *Mendeleev University of Chemical Technology, Moscow, 125047 Russia*
e-mail: salikhov@misis.ru

Abstract—The phase composition and structure of iron oxide nanopowders obtained by different chemical means are explored via X-ray diffraction, transmission electron microscopy, and Mössbauer and X-ray photoelectron spectroscopy. It is shown that nanoparticles with sizes of 10–85 nm are nonstoichiometric magnetite–maggemite compounds. Particles with average sizes of ~10 nm are close in composition and structure to (γ-Fe_2O_3) maggemite, while those with sizes above 70 nm resemble (Fe_3O_4) magnetite. Estimates of the magnetite particle size yield a value of 130 nm, which may be considered the conditional boundary from the bulk state to nanoscale effects.

DOI: 10.3103/S1062873815090166

INTRODUCTION

Growing attention is now being given to the study of magnetic nanoparticles based on iron oxide (magnetite and maggemite) [1, 2], due to the unique combination of their physicochemical characteristics and wide range of potential applications (e.g., magnetic liquids [3], nanocomposite magnetic materials [4], biosensors [5], MRI contrast agents [6], biomarkers [7], targered drug delivery [8], and local hyperthermy of tumors [9]).

Magnetite (Fe_3O_4) is a complex iron oxide that consists of bi- and trivalent iron ions. In the bulk state, it is a ferromagnetic with a Curie temperature of 585°C and a saturation magnetization of 80–100 A m^2 kg^{-1} at 300 K [10]. Magnetite has an enriched spinel structure (*Fd3m* spatial group) with 32 oxygen atoms (8 formula units) per unit cell, forming a FCC lattice with parameter $a = 0.8397$ nm, in which Fe^{+2} ions and half of the Fe^{+3} ions occupy octahedral (*B*) pores, while the other half occupy tetrahedral (*A*) pores [11–13] and is described by the crystallographic formula $(Fe_8^{3+})_A[Fe_8^{2+}Fe_8^{3+}]_BO_{32}$ (Fig. 1a). Maggemite (γ-Fe_2O_3) is a metastable form of Fe_2O_3 oxide, a ferromagnetic with a high Curie temperature (about 620°C) and saturation magnetization of 60–80 A m^2 kg^{-1} at 300 K. Unlike magnetite, maggemite contains only trivalent Fe^{3+} ions and is a phase with a cubic lattice, parameter $a = 0.83474$ nm ($P4_332$ spatial group), and homogeneously distributed vacances [14] (Fig. 1b). Maggemite can in essence be considered Fe^{+2} deficite magnetite in which 21 1/3 Fe^{3+} ions are distributed between 8 tetrahedral and 16 octahedral lacunes, and 2 2/3 vacancies (12.5%) remain in octahedral positions and are distributed statistically. As a result, γ-Fe_2O_3 can be described by the crystallographic formula $(Fe_8^{3+})_A[Fe_{40/3}^{3+}\phi_{8/3}]_BO_{32}$, where ϕ denotes a vacancy [15].

As can be seen, the γ-Fe_2O_3 structure is very close to that of Fe_3O_4; in addition, maggemite is metastable to gematite and forms a continious series of solid solutions with magnetite that makes their unequivocal identification via X-ray diffraction difficult, especially in the nanoscale state [2, 16]. This problem remains of great interest, and solving it will allow us not only to establish the structural and phase transformations that occur in iron oxide on the nanoscale level, but also to manage their phase composition and thus magnetic properties during their synthesis.

Complex studies of morphology, phase composition, and structure were performed in this work to investigate the structural and phase states in iron oxide nanopowders with dispersities of 10–85 nm, obtained by different chemical means. X-ray diffraction

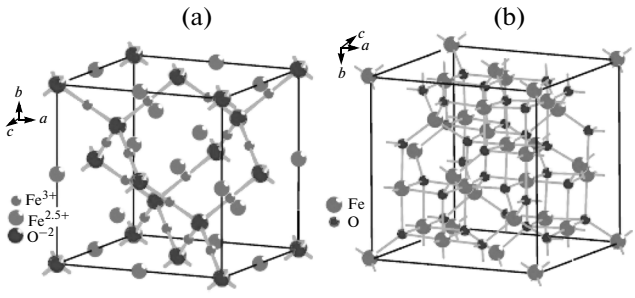

Fig. 1. Structures of (a) magnetite- and (b) maggemite-enriched spinel (H1.1 structural type) [14].

(XRD), transmission electron microscopy (TEM), nuclear gamma resonant and X-ray photoelectron spectroscopy (NGRS and XRPES, respectively) were used for this purpose.

EXPERIMENTAL

Iron oxide nanopowders with different dispersities were obtained via co-deposition (average size, ~10 nm), deposition (average size, 20–30 nm) and modified aging (sizes, >60 nm) [17, 18]. The sizes and shapes of the iron oxide nanoparticles, including the direct resolution of the crystalline lattice, were studied via TEM using a JEM-2100 microscope at an accelerating voltage of 200 kV. Carbon films with round holes on copper grids were used as substrates for our samples.

XRD was performed via powder diffractometry on an automized DRON-4 diffractometer in the Bregg–Brentano recording geometry, using CoK_α radiation with a graphite monochromator on the reflected beam. Quantitative phase analysis was performed and the sizes of coherent scattering domains were determined using the PHAN% software developed at the Department of Physical Material Science, National Research Technological University, according to the technique described in [19].

Our NGRS (Mössbauer) studies of ^{57}Fe nuclei were conducted at room temperature on a MS-1104Em spectrometer in transmission geometry using a ^{57}Co radiation source in a Rh matrix. Effective magnetic fields H_{eff} on the ^{57}Fe nuclei, isomeric shifts δ_s, and quadrupole splittings Δ of the elemental spectra, along with the relative intensity (area) of the latter, were determined by processing the Mössbauer spectra. The error in measuring H_{eff} was ±5 kE (0.4 MA m^{-1}). For δ_s, it was 0.01–0.02 mm s^{-1}; for Δ, it was ±0.01 mm s^{-1}; for the component area, it was ±0.6%.

The ionic composition of iron oxide nanopowders was studied via XRD on a PHI 5500 ESCA spectrometer. Monochromatic AlK_α radiation with a power of 210 W was used to excite photoemission and analyze standard Fe_2O_3 powder. The surface state of samples was studied at a redisual pressure in the chamber of less than 10^{-7} Pa after preliminary purification of the surface with Ar^+ ions. The error in determining the bivalent iron fraction via XRD was no greater than 10%.

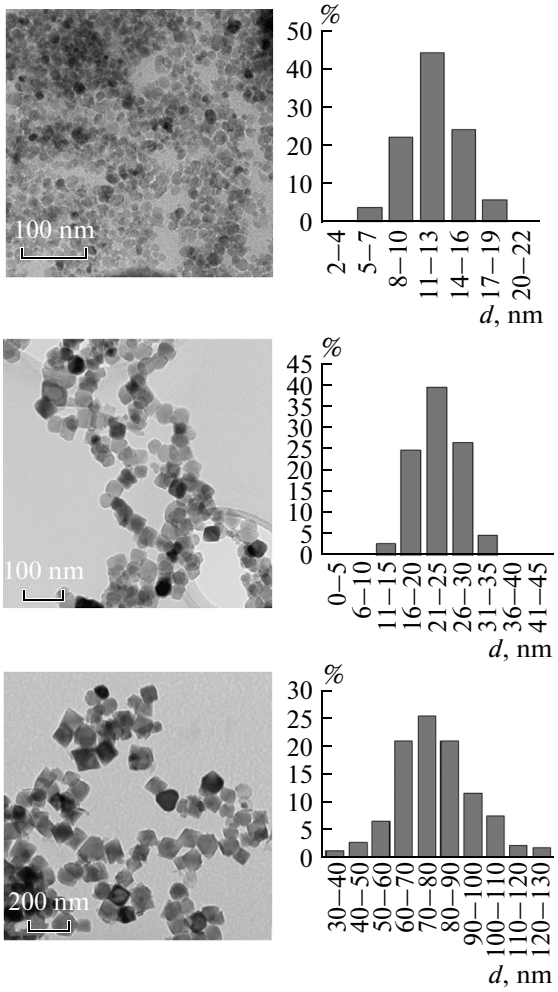

Fig. 2. Optical micrographs and relevant particle size distributions for iron oxide nanopowders prepared via (a) co-deposition, (b) deposition and (c) aging.

RESULTS AND DISCUSSION

Electron Microscopy Studies

As can be seen in Fig. 2, the iron magnetic oxide nanoparticles obtained by different means had different sizes (average values $\langle d \rangle$ are shown in Table 1). The particle size distributions calculated from the TEM optical micrographs (Fig. 2) displayed the expected profile in all cases.

Table 1. Results from our electron microscopy and X-ray diffraction (Rietveld) studies of iron oxide nanopowders

Method of synthesis	Lattice period, nm	Average geometric nanoparticle size $\langle d \rangle$, nm	Average size $\langle D \rangle$ of coherent scattering domains (CSDs), nm
Co-deposition	0.8361 ± 0.0004	10 ± 2	11 ± 2
Deposition	0.8368 ± 0.0004	25 ± 3	28 ± 5
Aging	0.8371 ± 0.0004	60 ± 4	56 ± 6
	0.8376 ± 0.0004	70 ± 5	63 ± 8
	0.8383 ± 0.0004	85 ± 6	65 ± 8

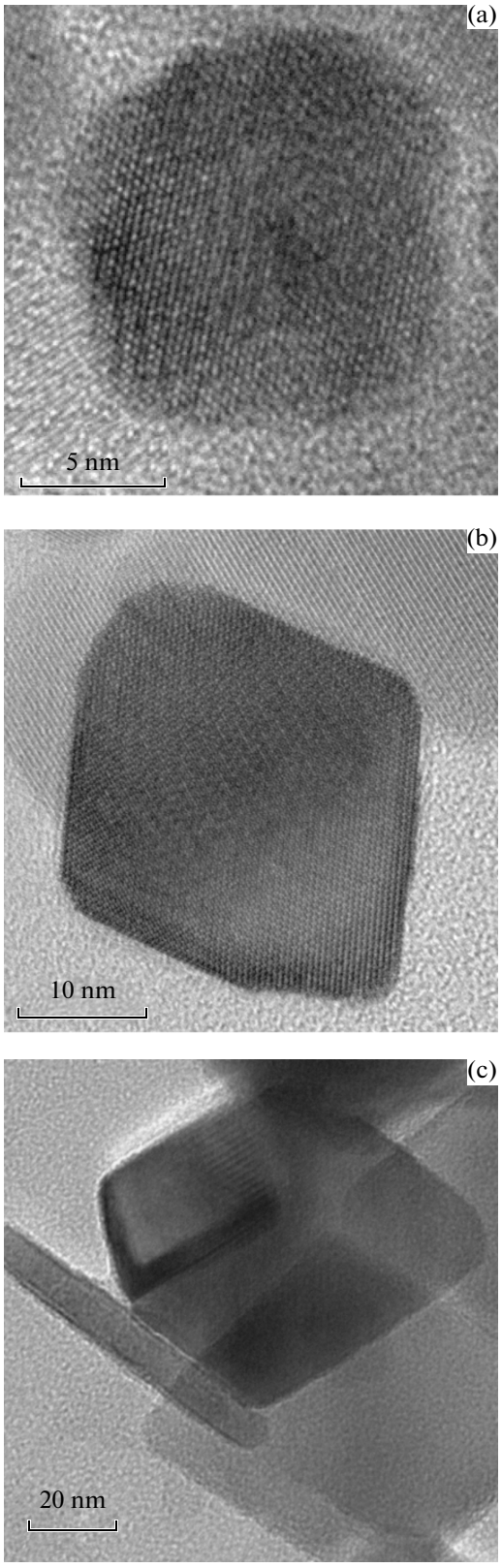

Fig. 3. High-resolution electron microscopy optical micrographs of iron oxide nanoparticles synthesized via (a) co-deposition, (b) deposition, and (c) aging.

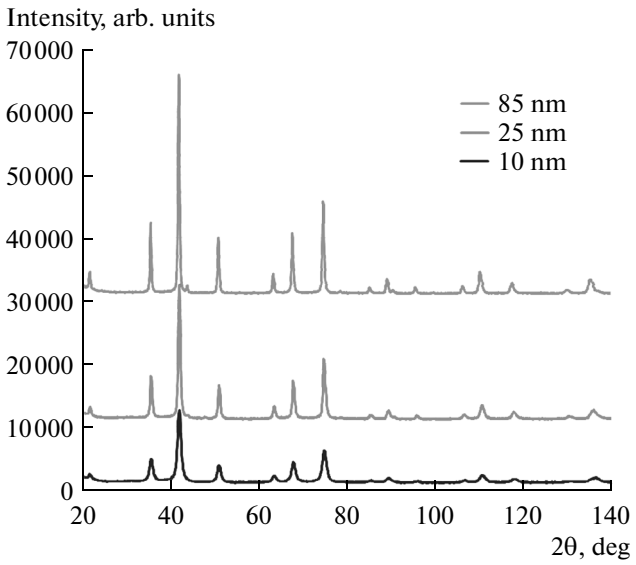

Fig. 4. X-ray diffraction patterns of iron oxide nanopowders synthesized via co-deposition (10 nm), deposition (25 nm), and aging (85 nm).

Our direct resolution electron microscopy studies (Fig. 3) showed the effect the method of synthesis (or size) had on the shape of iron oxide nanoparticles. The particles prepared via co-deposition were close to uniaxial in shape (Fig. 3a), while those obtained by deposition and aging had faceting; in addition, their shape became more anisotropic as their size grew; i.e., they took the form of cut plates (Fig. 3c).

X-ray Studies

Our XRD results for iron oxide nanopowders synthesized via co-deposition, deposition, and aging are presented in Fig. 4.

To analyze the experimental spectra, we selected those of the Fe_3O_4 and γ-Fe_2O_3 phases (belonging to the same H1.1 structural type) as our models. However, since the experimental and model spectra were in both cases almost identical, the latter are not shown in Fig. 4. At the same time, it is clear from Fig. 4 that the XRD profiles of all the investigated powders were typical of the single-phase state. This can be seen from the lack of asymmetry of the (511) line characteristic of the biphasic (magnetite–maggemite) state [21]. Their only important difference is the broadening of the diffraction lines, which diminishes as the size of the iron oxide nanoparticles grows.

If we compare the lattice periods calculated using the Rietveld method (Table 1) and those shown above for stoichiometric magnetite and maggemite, it is difficult to answer the question of which of these phases is present in the nanopowders. The powders obtained via co-deposition had a lattice period that was close to maggemite's but was comparable to magnetite's for

the powders prepared by aging. In the first case, however, it was greater than the values in the table and lower than them in the second.

In fitting the model spectra to the experimental ones, we determined the lattice periods of the phases and estimated average size $\langle D \rangle$ of the coherent scattering domains in the studied powders. Our results are presented in Table 1.

As can be seen from Table 1, average geometric size $\langle d \rangle$ of the nanoparticles and average size $\langle D \rangle$ of the coherent scattering domains in the studied powders agree with each other only for powders obtained via co-deposition and deposition, while the larger particles prepared via aging display a systematic reduction in the $\langle D \rangle$ values as the average particle size grows. There is a physical explanation for this: It confirms in particular the increased non-uniaxiality for iron oxide nanopowders prepared by aging that was established earlier via TEM as they grew. Summarizing the electron microscopy and X-ray diffraction results, we arrived at two conclusions: First, the average size of a coherent scattering domain and that of a nanoparticle are in fact identical. In other words, the studied powders are monocrystalline. Second, X-ray diffraction studies alone are not enough to determine correctly the sizes of the anisotropic nanocrystallites.

Mössbauer Studies

As is well known [21–23], the Mössbauer spectra from the ^{57}Fe nuclei in the Fe_3O_4 magnetite and γ-Fe_2O_3 maggemite lattices differ notably, and we might therefore expect that Mössbauer studies would help us answer the question of which of these phases was present in the studied samples.

Figure 5 shows the room-temperature Mössbauer spectra of iron oxide nanopowders synthesized via different chemical methods. Effective magnetic fields H_{eff} on the ^{57}Fe nuclei, isomeric shifts δ_s and quadrupole splittings Δ of the elementary spectra, and the relative intensities of the latter are shown in Table 2.

As is obvious from Table 2, the number of experimental spectrum components falls as the average particle size grows (i.e., the number of nonequivalent atomic configurations around the Fe atoms decreases). A sextet (sextet 4) whose characteristics were close to those of the α-FeOOH goethite phase was detected in iron oxide nanopowders prepared via co-deposition and deposition. Considering the nature of this means of synthesis, we may assume this phase was a thin film on the nanopowder surface; its thickness was estimated as 0.45–0.5 nm [24]. It therefore was not seen in the relevant X-ray diffraction spectra (the film was too thin) or in the Mössbauer spectra (the volume phase fraction was too small) of nanopowders with particle sizes of 60 nm or more.

The first three sextets can be attributed to the three nonequivalent arrangements of the Fe^{3+} and Fe^{2+} ions

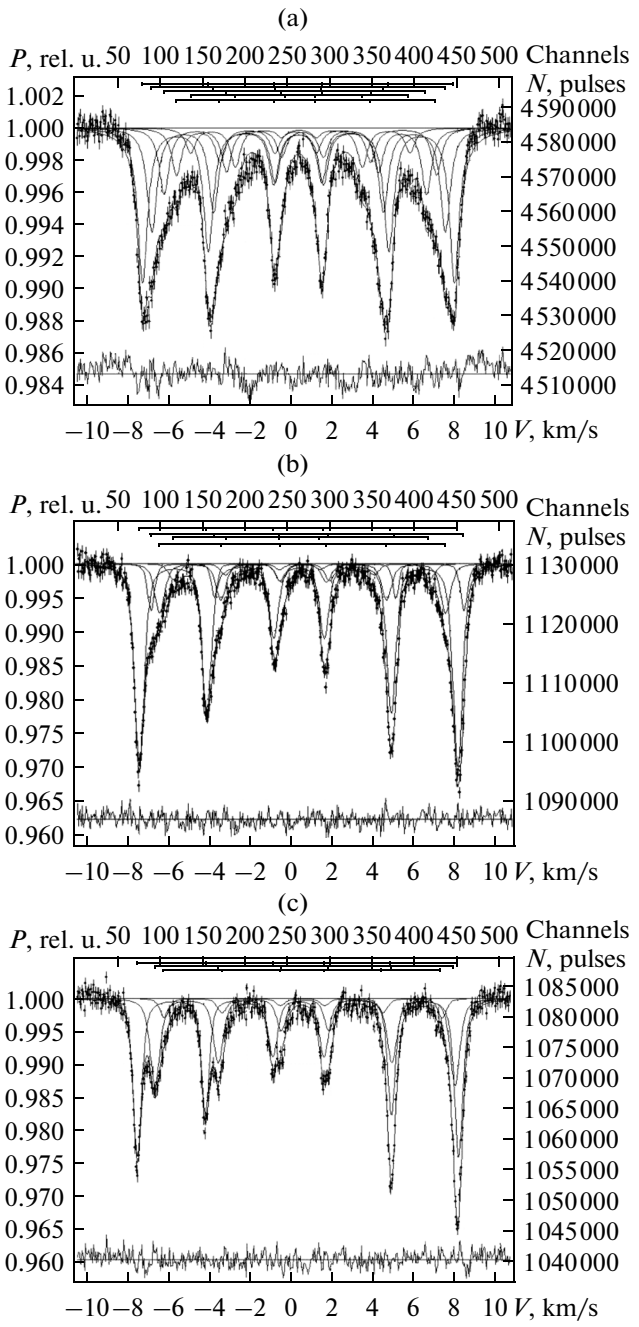

Fig. 5. Mössbauer spectra of nanopowders synthesized via (a) co-deposition, (b) deposition, and (c) aging.

in the tetra- and octahedral positions of the magnetite (sextets 1 and 2 for Fe ions in the tetra- and octahedral positions, respectively) and maggemite (sextet 3) lattices [21–23, 25]. We may also assume that the parameters' deviations from the corresponding values typical of the bulk state were due to the particles' small sizes and their structural features.

Analysis of the first three sextets using the technique described in [26] revealed that these Mössbauer spectrum components could be attributed to the three

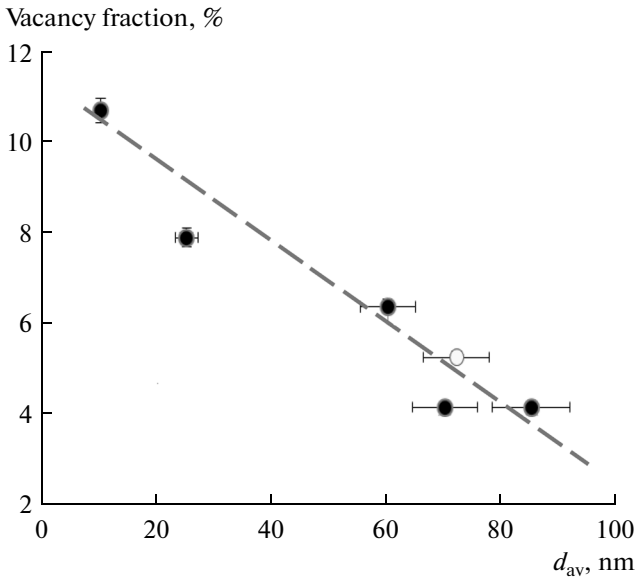

Fig. 6. Change in fraction of vacancies, depending on the average particle size in iron oxide nanopowders (the dashed line shows our extrapolation).

nonequivalent positions of Fe^{3+} and Fe^{2+} ions in the magnetite with a nonstoichiometric composition [27], the crystallographic formula of which can be described as $Fe^{3+}[Fe^{2+}_{1-3x}Fe^{3+}_{1+2x}\phi_x]O_4$, where ϕ and x are the denotation and formula coefficient of vacancies.

A feature of the Mössbauer spectra of nonstoichiometric magnetite is the disruption of electron exchange between Fe^{3+} and Fe^{2+} ions in the octahedral *B*) positions in the presence of vacancies. The fraction of the Fe^{3+} ions not involved in electron exchange due to the deficit of the Fe^{2+} ions makes an additional contribution in the Mössbauer spectra of the Fe^{3+} ions in tetrahedral (*A*) positions. If we consider the probabilities of the resonant effect for iron ions in positions *A* and *B* to be equal, the S_A/S_B ratio is

$$\frac{S_A}{S_B} = \frac{1 + 4.7x}{0.94(2 - 6x)}, \quad (1)$$

where x is the formula vacancy coefficient, while S_A and S_B are the areas of the Mössbauer spectra of the Fe^{3+} ions in the tetrahedral and octahedral positions.

It is follows from Eq. (1) that formula vacancy coefficient x is determined by the ratio

$$x = \frac{1.88\dfrac{S_A}{S_B} - 1}{4.7 + 5.64\dfrac{S_A}{S_B}}. \quad (2)$$

Using expression (2), we calculated the formula vacancy coefficients and determined the crystallographic formulas for nonstoichiometric magnetite; we also found the fractions of bivalent iron and vacancies for each studied sample. The vacancy fractions in the iron oxide nanopowders with different dispersions are shown graphically in Fig. 6.

Table 2. Parameters of the Mössbauer spectra from the ^{57}Fe nuclei of iron oxide nanopowders synthesized by different means

	H_{ef}, kE, MA m^{-1}	δ_s, mm s^{-1}	Δ, mm s^{-1}	Area of component, %
Co-deposition ($\langle d \rangle = 10$ nm)				
Sextet 1	477 (38.2)	0.33	–0.01	34
Sextet 2	450 (36.0)	0.32	–0.03	26
Sextet 3	416 (33.3)	0.33	–0.05	19
Sextet 4	377 (30.2)	0.38	–0.26	13
Sextet 5	331 (26.5)	0.29	–0.06	8
Deposition ($\langle d \rangle = 25$ nm)				
Sextet 1	484 (38.7)	0.29	–0.03	71
Sextet 2	476 (38.1)	0.66	0.02	10
Sextet 3	435 (34.8)	0.51	–0.05	13
Sextet 4	390 (31.2)	0.39	0.09	6
Aging ($\langle d \rangle = 85$ nm)				
Sextet 1	490 (39.2)	0.31	–0.01	56
Sextet 2	458 (36.6)	0.64	–0.01	37
Sextet 3	424 (33.9)	0.54	0.01	7

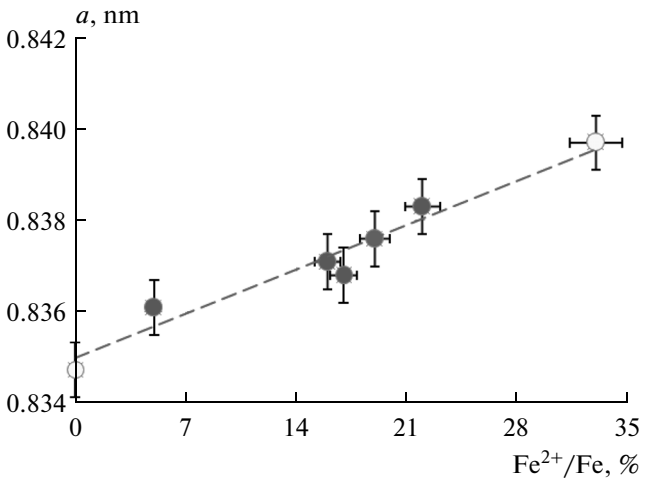

Fig. 7. Change in the lattice parameter of nonstoichiometric magnetite, depending on the bivalent iron fraction. The extreme points in the plot represent stoichiometric aggemite (a = 0.83474 nm; x = 0) and magnetite (a = 0.8397 nm; x = 0.33), repsectively.

We can see that with particle sizes below 20 nm, the crystallographic state was close to maggemite, while with those above 80 nm it was typical of magnetite. This was indirectly confirmed by the quasi-linear dependence shown in Fig. 7 for the calculated bivalent iron fraction in nonstoichiometric magnetite on the lattice parameter of the studied powders (Table 2).

Extrapolating the vacancy fraction as a function of the average particle size to zero (the dashed line in Fig. 6) shows that at average sizes of around 130 nm, the nanoparticles consist of only the magnetite phase. We may thus assume this size to be the conventional boundary from the bulk to the nanoscale state.

XRD Studies

To verify our Mössbauer spectroscopy results, we made XRD measurements of the ion composition in iron oxide nanopowders obtained via deposition ($\langle d\rangle$ = 12 nm) and aging ($\langle d\rangle$ = 85 nm). The relative Fe^{2+} ion content (Fe^{2+}/Fe) was determined from the spectrum of Fe3p using the technique described in [28]. The results from approximating the experimental spectra are shown in Fig. 8. The spectrum of the standard Fe_2O_3 is presented there as well.

As can be seen in Fig. 8, the spectrum of the standard material also exhibits peak *1* associated with the Fe^{2+} ions, which presumably arose as a consequence of the partial reduction of Fe_2O_3 iron oxide to FeO during the ion etching of its surface. In light of this adjustment, we nevetheless established that the relative Fe^{2+}/Fe fraction in the sample prepared via deposition was 7%, while for the sample prepared via aging it was 22%. As is obvious in Fig. 9, these data are in good correlation with the results from our Mössbauer studies, thus proving the validity of our analysis.

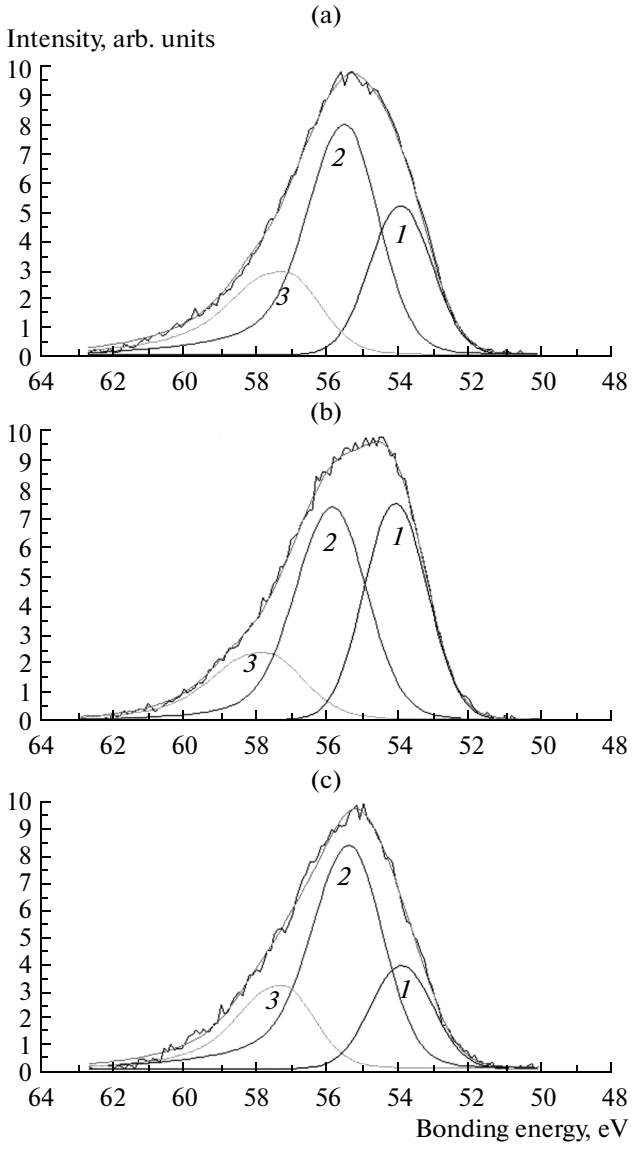

Fig. 8. Spectra of Fe3p after cleaning the samples prepared via (a) deposition and (b) aging, and (c) standard Fe_2O_3. Peak *1* represents the relative Fe^{2+}/Fe fraction; peaks *2* and *3* represent the relative Fe^{3+}/Fe fraction.

CONCLUSIONS

Our complex investigations of iron oxide nanopowders with average particle sizes of 10 to 85 nm synthesized by different chemical means allowed us to establish that they were a nonstoichiometric magnetite–maggemite compound described by the crystallographic formula $Fe^{3+}[Fe^{2+}_{1-3x}Fe^{3+}_{1+2x}\phi_x]O_4$, where ϕ and x are the denotation and formula coefficient of vacancies, respectively. Particles with average sizes of around

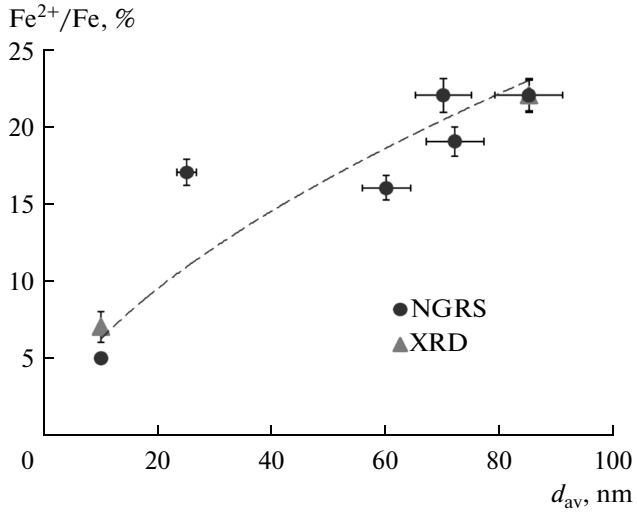

Fig. 9. Bivalent iron fraction as a function of the average nanoparticle size, according to our Mössbauer and XRD studies (the line is drawn for the sake of clarity).

10 nm were close in both composition and structure to maggemite, while larger ones resembled magnetite. The magnetite particle size that we may assume was the conventional boundary between the bulk and nanoscale state was approximately 130 nm. It was also established that iron oxide nanoparticles with sizes below 30 nm and prepared by chemical means were uniaxial and had on their surfaces films around 0.5 nm thick that were close in composition and structure to goethite (α-FeOOH). This film thinned as the average particle size grew and their faceting became more refined. This was not observed for particles with the average sizes above 30 nm, testifying to their chemical stability in the faceted state.

ACKNOWLEDGMENTS

We are grateful to the staff of the Faculty of Physical Material Science at MISiS for their help in preparing our nanopowders and conducting our structural investigations.

REFERENCES

1. Lukashova, N.V., Savchenko, A.G., Yagodkin, Yu.D., et al., *Metalloved. Term. Obrab. Met.*, 2012, no. 10, p. 60.
2. Savchenko, A.G., Salikhov, S.V., Yurtov, E.V., et al., *Bull. Russ. Acad. Sci.: Phys.*, 2013, vol. 77, no. 6, p. 704.
3. Beaucage, G., Mark, J.E., Burns, G.T., et al., *Nanostructured Powders and Their Industrial Application*, Warrendale, PA: Mater. Res. Soc., 1998.
4. Lyubutin, I.S., Lin, C.R., Korzhetskiy, Yu.V., et al., *J. Appl. Phys.*, 2009, vol. 106, no. 3, p. 034311.
5. Perez, J.M., Josephson, L., O'Loughlint, T., et al., *Nat. Biotechnol.*, 2002, vol. 20, p. 816.
6. Weissleder, R., Bogdanov, A., Neuwelte, E., et al., *Adv. Drug Delivery Rev.*, 1995, vol. 16, p. 321.
7. Pershina, A.G., Sazonov, A.E., and Mil'to, I.V., *Byull. Sib. Med.*, 2008, no. 2, p. 70.
8. Jurgons, R., Seliger, C., Hilpert, A., et al., *J. Phys.: Condens. Matter.*, 2006, vol. 18, p. 2893.
9. Neilsen, O., Horsman, M., and Overgaard, J., *Eur. J. Cancer*, 2001, vol. 37, p. 1587.
10. *Tablitsy fizicheskikh velichin* (Tables of Physical Quantities), Kikoin, I.K., Ed., Moscow: Atomizdat, 1976.
11. Vervey, E.J.W., *Nature*, 1939, vol. 144, p. 327.
12. Phase, D.M., Tiwari, S., Prakash, R., et al., *J. Appl. Phys.*, 2006, vol. 100, p. 123703.
13. Dorfman, Ya.G., *Magnitnye svoistva i stroenie veshchestva* (Matters Magnetic Properties and Structure), Moscow: Gostekhizdat, 1955.
14. Salazar-Alvarez, G., Synthesis, characterisation and applications of iron oxide nanoparticles, *Doctoral Thesis*, Stockholm, 2004.
15. Schwertmann, U. and Cornell, R.M., *Iron Oxides in the Laboratory*, Weinhem: VCH Verlagsgesellschaft, 1991.
16. Johnson, C.E., Costa, L., Gray, S., et al., *Proc. 36th Annu. Condensed Matter and Materials Meeting*, Wagga Wagga, 2012, p. FO01:1.
17. Elmore, W.C., *Phys. Rev.*, 1938, vol. 54, p. 309.
18. Massart, R., *IEEE Trans. Magn.*, 1981, vol. 17, p. 1247.
19. Shelekhov, E.V. and Sviridova, T.A., *Metalloved. Term. Obrab. Met.*, 2000, no. 8, p. 16.
20. Kim, W., Suh, C.-Y., Cho, S.-W., Roh, K.-M., et al., *Talanta*, 2012, vol. 94, p. 348.
21. Costa, G.M., Grave, E., Bakker, P.M., and Vandenberghe, R.E., *Clays Clay Miner.*, 1995, vol. 43, no. 6, p. 656.
22. Cannas, C., Concasa, G., Congiua, F., et al., *Z. Naturforsch., A: Phys. Sci.*, 2002, vol. 57, p. 154.
23. Suzdalev, I.P., *Dinamicheskie effekty v gamma-rezonansnoi spektroskopii* (Dynamical Effects in Gamma-Resonance Spectroscopy), Moscow: Atomizdat, 1979.
24. Yagodkin, Yu.D., Salikhov, S.V., and Ushakova, O.A., *Zavod. Lab. Diagn. Mater.,* 2013, vol. 79, no. 4, p. 41.
25. *Khimicheskie primeneniya messbauerovskoi spektroskopii* (Chemical Applications of Mossbauer Spectroscopy), Gol'danskii, V.I., Krizhanovskii, L.I., and Khrapov, V.V., Eds., Moscow: Mir, 1970.
26. Da Costa, G.M., Blanko-Andujar, C., De Grave, E., and Pankhurst, Q.A., *J. Phys. Chem. B*, 2014, vol. 118, p. 11738.
27. Kamali, M.S., Ericsson, T. and Wappling, R., *Characterization of Iron Oxide Nanoparticles by Mössbauer Spectroscopy*, Uppsala: Uppsala Univ., 2010.
28. Yamachita, T. and Hayes, P., *Appl. Surf. Sci.*, 2008, vol. 254, p. 2441.

Translated by O. Maslova